NASA TN D-3245

IMPULSE AND THRUST TEST OF A SUBLIMATING-SOLID MICROPROPULSION SYSTEM

By Richard W. Forsythe

Goddard Space Flight Center
Greenbelt, Md.

NATIONAL AERONAUTICS AND SPACE ADMINISTRATION

For sale by the Clearinghouse for Federal Scientific and Technical Information
Springfield, Virginia 22151 – Price $2.00

ABSTRACT

An integrating microthrust balance was utilized to evaluate the impulse and thrust performance characteristics of a rocket system which employs a new concept for propulsion; that is, it effects a controlled thrust from the sublimation of a solid propellant. The propulsion package tested was designed to provide thrust in a control system of a spin stabilized satellite.

CONTENTS

IMPULSE AND THRUST TEST OF A SUBLIMATING-SOLID MICROPROPULSION SYSTEM

by
Richard W. Forsythe
Goddard Space Flight Center

INTRODUCTION

This report describes the initial tests conducted by Goddard Space Flight Center on a micro-thrust attitude control rocket system which employs a new concept; that is, it utilizes a sublimating solid propellant as a means for propulsion. The system tested was designed and fabricated on NASA contract NAS5-3153 by Rocket Research Corporation of Seattle, Washington. The concept of the propulsion developed as a result of in-house R&D work by the same contractor.

There are a large number of applications for very low thrust systems in satellite missions. Until now, the only operational hardware systems available utilized cold gas nitrogen as the propellant. Cold gas nitrogen has the major disadvantages of (a) high weight due to low density of the propellant and high pressure of the fuel tank and (b) reduced reliability of the system due to multiplicity of high pressure moving parts such as pressure regulators and control valves.

The sublimating solid microrocket is an improved cold-gas reaction jet system, which maintains cold gas simplicity while reducing system component weight and increasing reliability. The sublimating solid microrocket has a theoretical vacuum specific impulse of 85 seconds at 70°F when expanded through a nozzle with a 40 to 1 area ratio. Physically, the system consists of a thin wall propellant tank, a sublimating solid propellant in crystal form, a filter, a propellant valve, and a nozzle. The resulting control rocket is one of the simplest systems possible. When the valve is opened, the vapor escapes through the nozzle to produce thrust. The solid sublimes to replace the vapor which has been released. The use of the sublimating solid propellant does not involve ignition, combustion, or high temperature and high pressure. Therefore, no reaction chambers, pressure regulators, or high pressure storage tanks are required. Since the propellant is stored in solid form and the vapor pressure of the propellant is low, the propellant tank weight for the sublimating solid microrocket is very low, in direct contrast to the cold-gas nitrogen system in which tank weight often exceeds propellant weight. Low system operating pressure also reduces leakage problems and results in high overall reliability for the system.

TEST SYSTEM DESCRIPTION

The NASA specifications for the propulsion system were selected such that the operating characteristics met the requirements of a spinning-satellite-pointing controls mechanism in all

respects except weight. The components were designed for laboratory testing only and no attempt was made to minimize weight. The sublimating-solid propulsion system tested is shown assembled in Figure 1.

The total weight of the laboratory system was 2.67 pounds with approximately 1.6 pounds of fuel. The valve utilized was an axial solenoid poppet type valve.

The fuel utilized was selected considering the following criteria:

1. The propellant material must possess a significant vapor pressure (in relation to the desired thrust level).
2. The melting or decomposition points cannot be too low.
3. The molecular weight of the exhaust gases should be as low as possible to achieve a high specific impulse.
4. The propellant density should be as high as possible to reduce storage area and weight.
5. The heat of sublimation of the solid fuel should be as low as possible to allow higher impulse bits.

From a number of possible fuels, ammonium hydrogen sulfide (NH_4HS) was selected as the fuel. Ammonium hydrogen sulfide has a heat of sublimation of 782 Btu/lbm and a density of approximately 0.03 lbm/in^3. Upon sublimation it decomposes into ammonia (NH_3) and hydrogen sulfide (H_2S) with an average molecular weight of 25.6. The gases have a distinct and pungent odor; although high concentrations are toxic, due to their low threshold of olefactory sensitivity, they are easily detected long before the concentrations are sufficient to be dangerous. Figure 2 shows the equilibrium conditions for ammonium hydrogen sulfide on a pressure versus temperature curve.

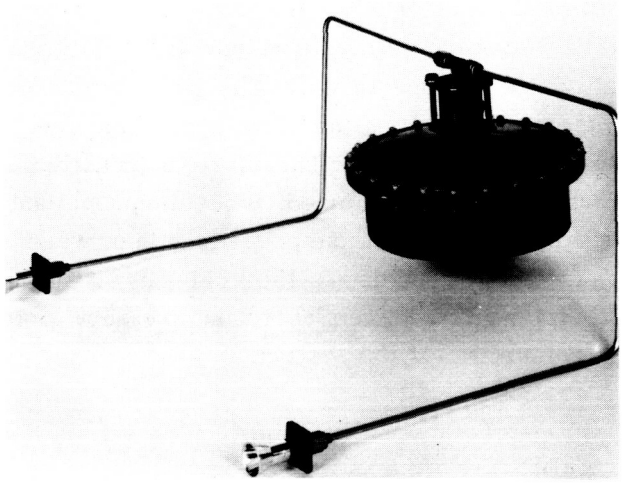

Figure 1—Assembled sublimating-solid micropropulsion system.

Table 1

System Specifications.

Parameter	Specification
Total Thrust (2 nozzles)	5×10^{-2} lbf (nominal)
Specific Impulse	83 lbf-sec/lbm (theoretical)
Inlet Nozzle Pressure	1.80 psia (nominal)
Tank Pressure	6.35 psia (nominal)
Total Mass Flow	6.04×10^{-2} lbm/sec (nominal)
Thrust Coefficient	1.80 (theoretical)
Throat Area	7.85×10^{-3} in^2
Area Ratio	40

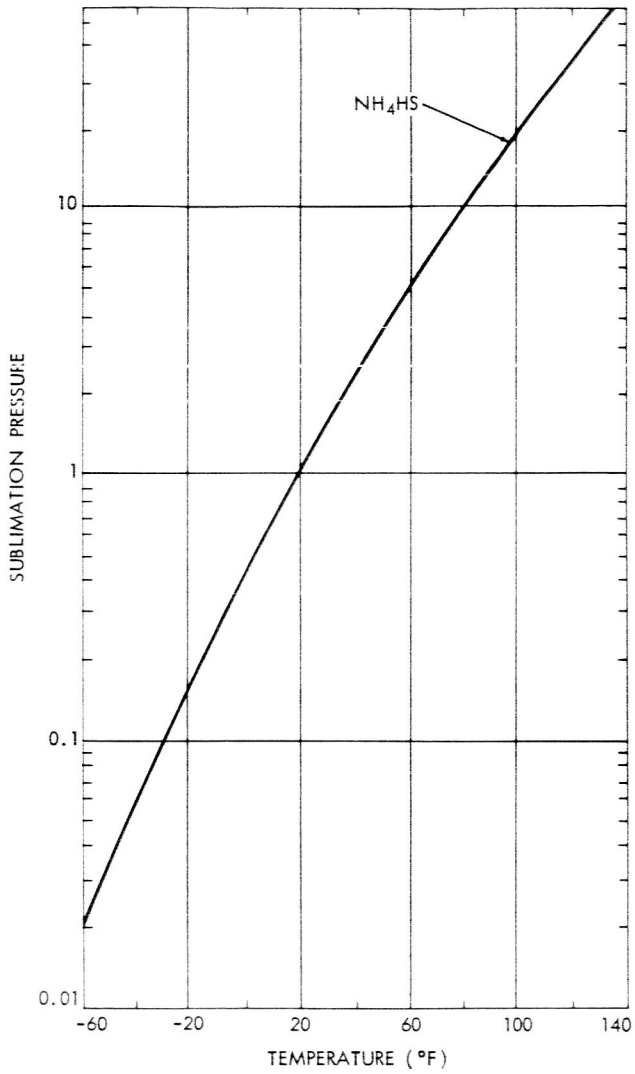

Figure 2—Sublimation pressure versus temperature.

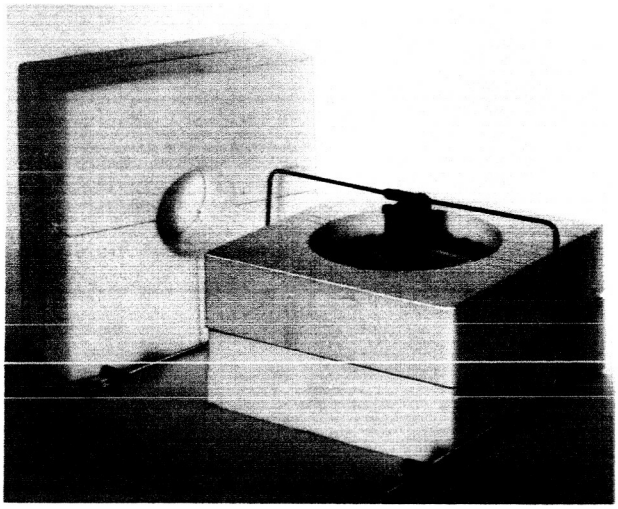

Figure 3—Fuel tank for sublimating-solid micropropulsion system and its styrofoam tank container.

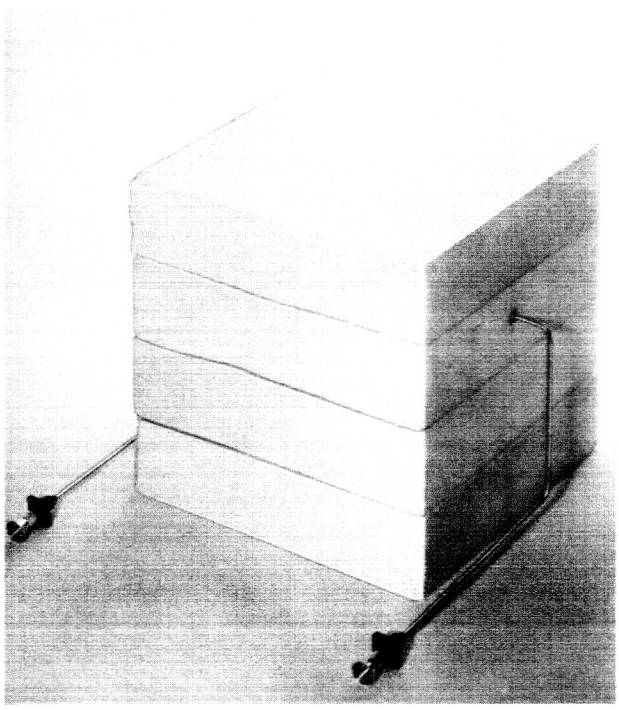

Figure 4—Styrofoam container completely enclosing fuel tank.

TEST PLAN

The purpose of the test was to evaluate the thrust and impulse delivered from the propulsion system which had been stored with its fuel in a refrigerator system at 34°F for 8 months. To eliminate the extraneous thermal environment around the test system during the tests, the fuel tank and valve were essentially thermally isolated by mounting them inside a styrofoam container. Figures 3 and 4 illustrate the test arrangement.

To achieve the desired temperatures during the test, heater strip wiring was wrapped directly around the fuel tank and valve and supplied with power upon command external to the vacuum

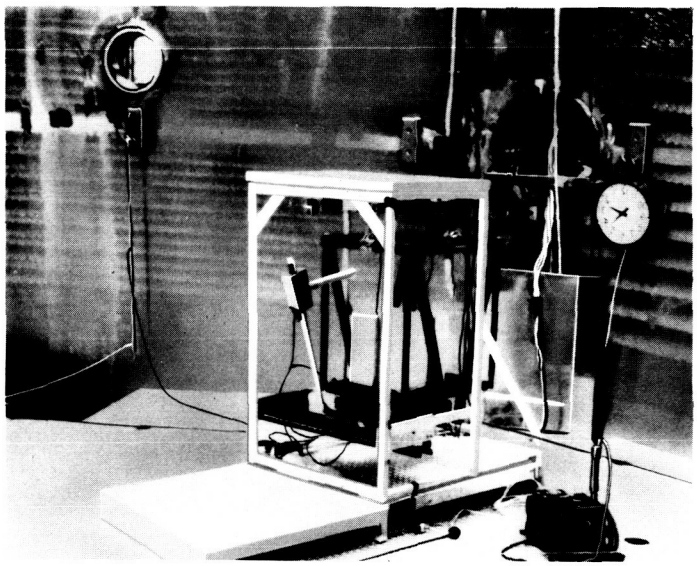

Figure 5—Sublimating-solid micropropulsion system on integrating microthrust balances.

chamber. Thermocouples fed into the styrofoam box system to allow temperature monitoring. The valve temperature was kept above the fuel temperature at all times to insure against any gas recondensation at the valve.

To accurately measure the thrust and impulse, the propulsion system was mounted on an Integrating Microthrust Balance, (IMB) in a vacuum chamber (Figure 5). The IMB, which utilizes a *soft* suspension, is basically a linear displacement pendulum designed and instrumented to measure momentum imparted to it by a single pulse bit.

The IMB is calibrated by instantaneously applying a known momentum to the pendulum; because the propulsion system is not an instantaneous application of total momentum, a slight error in readout develops with the amount directly related to the impulse time. Analysis, however, allows the development of correction factors to compensate for the impulse time and also drag of the pendulum due to a damping system. All data shown has been adjusted slightly by a correction curve. Appendix A gives a complete description of the IMB and the analysis which develops the correction curve.

Once the test system and equipment was set up as shown in Figure 5, the vacuum chamber was pumped down to 2×10^{-2} mm of Hg at which pressure three tests were conducted to evaluate the thrust and impulse of the system as follows:

Test 1 — The propulsion system valve was energized and the system allowed to deliver a steady state thrust for 18.33 seconds.

Test 2 — Power to the solenoid valve was delivered by a timing circuit external to the chamber which allowed the system to pulse for 250 milliseconds every 3 seconds for 40 pulses.

Test 3 — By the timing circuit, the system was pulsed with varying pulse bits 250, 200, 150, 100 and 77 milliseconds in duration.

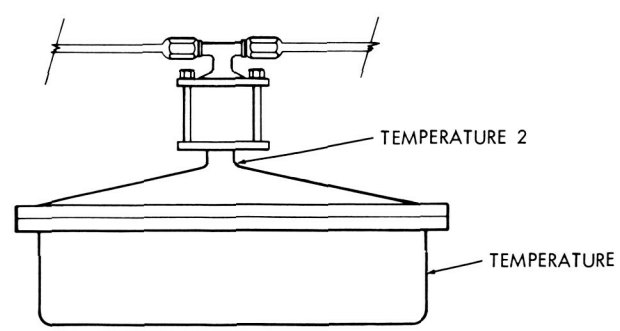

Figure 6—Location of thermocouples on fuel tank.

Two thermocouples at the positions indicated in Figure 6 monitored the temperature during all tests.

TEST RESULTS AND ANALYSIS

The following test results and analysis deal with the impulse and thrust data after it was reduced and adjusted by the IMB procedure discussed in Appendix A.

Test 1

A power supply external to the chamber supplied 28.0 volts to the solenoid valve for 18.33 seconds. This allowed the propulsion system to deliver a steady state thrust which displaced the IMB pendulum. The test record of displacement versus time is shown in Figure 7.

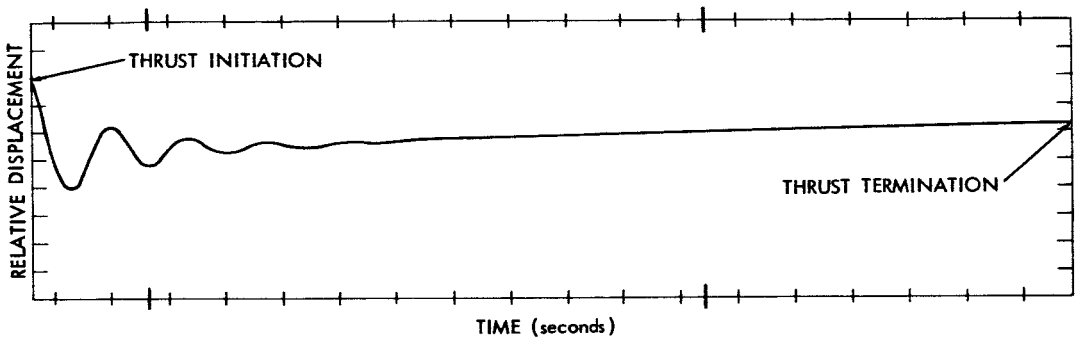

Figure 7—Plot of relative displacement versus time for steady-state thrust.

Extrapolating the steady-state thrust displacement back to time = 0 seconds, an initial relative displacement of 2.28 is obtained. The final relative displacement is 1.40.

The equation of motion describing the thrust balance motion is

$$m\ddot{x} + c\dot{x} + kx = F(t) . \quad (1)$$

Under the influence of a steady state forcing function independent of time where the damping, c, is appreciable, the resultant displacement is described by

$$kx = F \text{ when } \ddot{x} \text{ and } \dot{x} \text{ approach } 0 . \quad (2)$$

Utilizing this fact and the dynamics of the IMB (see Appendix A for deviation of thrust levels) the thrust levels at thrust initiation and termination were obtained.

Table 2 presents the Test 1 data. The terminal temperatures shown were the lowest values of the temperatures and were reached at approximately T + 125 seconds as indicated.

Table 2

Test 1 Data.

Time (seconds)	Relative Displacement	Thrust, 2 nozzles, (lbf)	Temp No. 1 (°F)	Temp No. 2 (°F)
0	2.28	0.068	73.4	87.0
18.33	1.40	0.042	----	----
125.00	----	-----	60.8	78.0

The reduction in thrust from 0.068 lbf to 0.042 lbf of 38.3% is attributed solely to the temperature drop of the system through the following reasoning. Utilizing the well-known formula for thrust, F, through a nozzle, the total thrust for our system of two identical nozzles is

$$F_{total} = \left[C_f A_t P_c\right]_{nozzle\ 1} + \left[C_f A_t P_c\right]_{nozzle\ 2} , \tag{3}$$

where

C_f = the thrust coefficient of the nozzles,

A_t = the nozzle throat area,

and

P_c = the absolute tank chamber pressure.

Since C_f and A_t are constant for a given system, thrust varies directly with the absolute tank chamber pressure; i.e.,

$$\frac{F}{P_c} = 2 C_f A_t = \text{constant} .$$

Therefore, if a thrust, F_1, at a tank temperature, T_1, is known and it is desired to know the thrust, F_2, at any temperature, T_2, this may be calculated by

$$F_2 = \frac{P_{c2}}{P_{c1}} F_1 , \tag{4}$$

where the chamber pressures P_{c2} and P_{c1} are obtained by knowing the temperatures and utilizing the equilibrium chart (Figure 2) for the fuel. Therefore, it is seen that as the temperature drops, the thrust drops, and vice versa.

The explanation of the temperature drop and its extent is as follows: Since the reduction in balance displacement was approximately linear, by assuming a delivered specific impulse, I_{sp}, of 83 lbf-sec/lbm, the approximate weight of fuel w_f, used, was

$$w_f = \int_0^t \dot{w}_f \, dt \approx \frac{F}{I_{sp}} \int_0^t dt$$

$$= \frac{(0.068 + 0.042)\ \text{lbf}}{2(83\ \text{lbf-sec/lbm})} (18.33\ \text{sec}) = 0.012\ \text{lbm} . \quad (5)$$

The NH_4HS will attempt to stay on the equilibrium vapor pressure curve shown in Figure 2. When 0.012 lbm of gas vapor is pulsed out, the solid fuel sublimates to maintain its equilibrium vapor pressure. However, the heat of sublimation, h_{sg}, is 782 Btu/lbm and since the fuel tank was mounted inside of an 18" × 18" styrofoam container, the process may be considered essentially adiabatic. The tank and fuel must provide the sublimation heat; therefore, the fuel temperature, and thus equilibrium condition, was necessarily lowered. The heat necessary was

$$Q = (w_f)(h_{sg})$$

$$= (.012\ \text{lbm})(782\ \text{Btu/lbm}) = 9.38\ \text{Btu} . \quad (6)$$

By assuming that the required heat was obtained from the aluminum tank and NH_4HS fuel alone, the heat balance may be described by:

$$Q = \int_0^T w_t\, c_t \, dT + \int_0^T w_f\, c_f \, dT , \quad (7)$$

where

Q = total heat exchanged,

w_t = weight of the aluminum tank (0.610 lb),

c_t = specific heat of aluminum (0.214 Btu/lb. °F),

w_f = weight of NH_4HS fuel (1.600 lb),

and

c_f = specific heat of NH_4HS (0.340 Btu/lb. °F).

Assuming constant specific heats and weight of NH_4HS, and that the fuel and tank equalize at the same temperature, the change in temperature should have been approximately

$$\Delta T = \frac{Q}{w_t c_t + w_f c_f}$$

$$= \frac{9.380 \text{ Btu}}{(.610 \text{ lb})\left(.214 \frac{\text{Btu}}{\text{lb°F}}\right) + (1.610 \text{ lb})\left(.340 \frac{\text{Btu}}{\text{lb°F}}\right)} = 13.9°\text{F} .$$

From Table 2 it is seen that the tank temperature (temp. 1) actually dropped from 73.4°F to 60.8°F or 12.6°F.

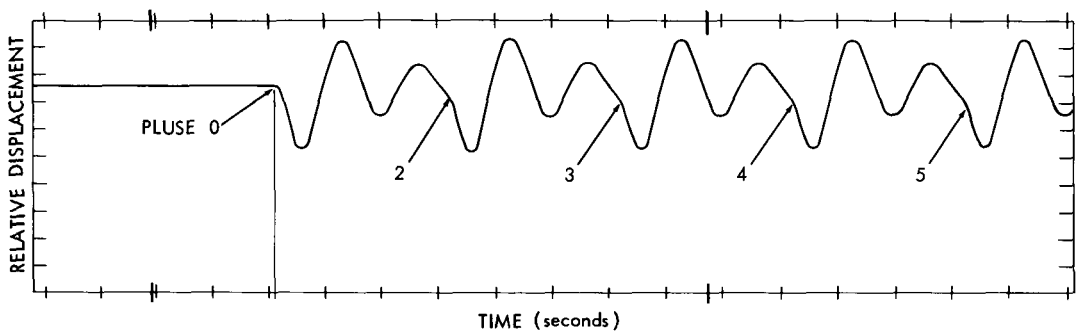

Figure 8—Plot of relative displacement versus time for 250-millisecond pulses every 3 seconds.

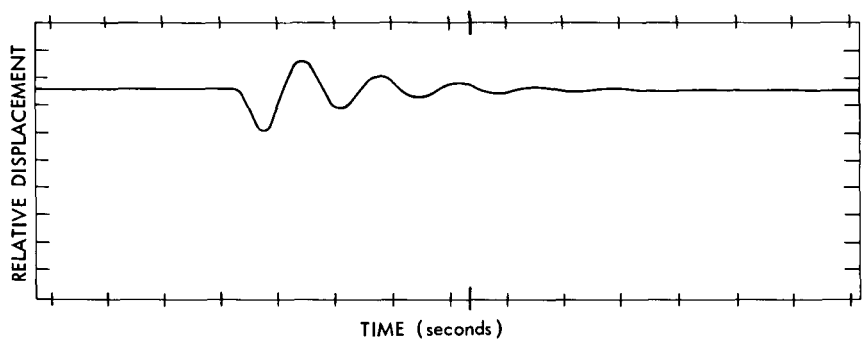

Figure 9—Plot of relative displacement versus time for a 250-millisecond pulse bit.

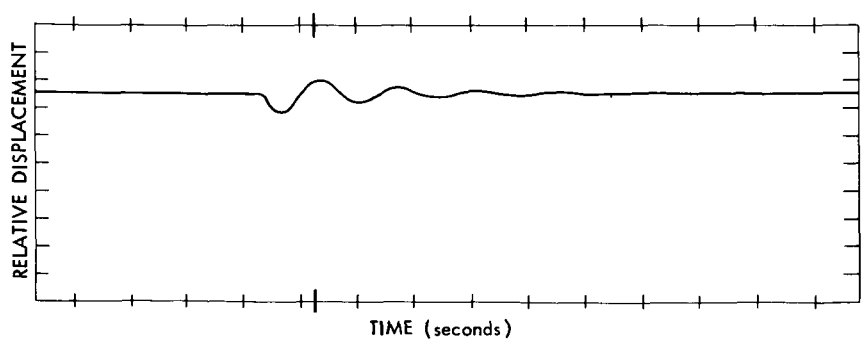

Figure 10—Plot of relative displacement versus time for a 77-millisecond pulse bit.

Test 2

The timing circuit external to the chamber supplied 28.0 volts to the solenoid valve for 250-millisecond pulses every 3 seconds for a total of 40 pulses. The purpose of this test was to simulate the propulsion system incorporated in the pointing controls in a spinning satellite and to investigate the reduction in thrust over approximately 2 minutes of operating time. The 3-second intervals simulated a satellite spin rate of 20 rpm and the 250-millisecond pulse simulated a controls system on time of 30° per rotation. The test record of the first six pulses on the IMB pendulum is shown in Figure 8.

To obtain the initial thrust the first swing relative displacement was measured for the first pulse, the total impulse delivered read off of the IMB pendulum calibration curve (see Appendix A), the impulse adjusted to correct for the extended pulse (see Appendix A), and the impulse divided by the pulse bit to give the average thrust. After the 39th pulse, a 20.8-second delay was interjected. This allowed the IMB pendulum displacement to completely damp out. The 40th pulse was then delivered. The relative displacement of the 40th pulse was utilized to indicate the final impulse and thrust. Table 3 tabulates the results of Test 2.

Again the terminal temperatures shown indicate the lowest values of temperature recorded and it was assumed equilibrium was obtained at that time.

From Table 3 it is observed that the average thrust dropped from 0.064 to 0.043, or 32.8%. Again, as in Test 1, it is attributed directly to the drop in temperature of the tank from 70.7°F to 60.8°F.

Table 3

Test 2 Data.

Pulse	Time (seconds)	Relative Displacement	Total Impulse (lbf-sec.)	Thrust, 2 nozzles (lbf)	Temp 1 (°F)	Temp 2 (°F)
1	0	2.26	.0159	.064	70.7	82.4
40	134.8	1.52	.0107	.043		
--	300.0	----	-----	----	60.8	73.5

Test 3

The timing circuit external to the vacuum chamber was utilized to supply 28.0 volts to the solenoid valve for six impulse bits verying in duration from 250 to 77 milliseconds. The record of 250 and 77-millisecond pulse bits are shown in Figures 9 and 10.

The impulses and thrusts were reduced from the IMB calibration curve as described in Appendix A. Table 4 summarizes the results of test 3.

Table 4

Test 3 Data.

Pulse	Pulse Bit Duration (milliseconds)	Relative Displacement	Total Impulse (lbf-sec.)	Thrust, 2 nozzles (lbf)	Temp 1 (°F)	Temp 2 (°F)
1	250	1.50	0.0106	0.042	63.5	75.2
2	200	1.29	0.0089	0.045	64.4	75.2
3	150	1.05	0.0071	0.048	65.3	78.8
4	100	0.80	0.0054	0.054	68.0	82.4
5	77	0.68	0.0045	0.059	69.8	84.2
6	77	0.68	0.0045	0.059	69.8	84.2

Prior to pulse 1, the heater strip wiring was utilized to elevate the temperature of the fuel tank and valve. From Table 4 it is seen that the temperature continued to rise during the six pulses; this effected the increase in average thrust as indicated in the table.

POST TEST EXAMINATION

After the termination of the tests the propulsion system was left inside the vacuum chamber at 2×10^{-2} mm of Hg for approximately 24 hours. The chamber was then brought back up to atmospheric pressure and the propulsion system was removed, purged with dry nitrogen, and stored in a small air-tight can at 34°F.

Two weeks later the fuel system was taken out of storage for examination and the following was revealed:

1. The fuel vapors had attacked the black anodized surface of the aluminum tank causing a slight discoloration as may be seen in Figure 1.

2. The valve exterior surface was nickel plated over mild steel and had been attacked by the hydrogen sulfide forming a crust on the metal.

3. Disassembly of the valve revealed that there were brass components inside the valve which had been severely attacked by the hydrogen sulfide such as to render the valve inoperable.

Since the valve was operating at termination of the tests and none of the exterior effects were obvious when the propulsion system was removed from the vacuum chamber, it is surmised that the valve developed a leak near the end of the tests. Stored in the small can, the leak allowed high concentrations of the fuel vapor to come into contact with the exterior of the system and caused the corrosive attack. The existence of a leak, is further supported by the following analysis of the total fuel missing versus what should have been used.

The total impulse delivered by the fuel system during the three tests was

Test 1	1.009 lbf-sec
Test 2	0.535 lbf-sec
Test 3	0.041 lbf-sec
	1.585 lbf-sec

Therefore, the theoretical weight of fuel w_f used, was

$$w_f = \frac{\Sigma F \Delta t}{I_{sp}}$$

$$w_f = \frac{1.585 \text{ lbf-sec}}{83 \text{ lbf-sec./lbm}}$$

$$w_f = 0.019 \text{ lbm} ,$$

where

$\Sigma F \Delta t$ = the total impulse delivered,

and

I_{sp} = the specific impulse of the fuel.

The actual fuel used during the period while the propulsion system was inside the vacuum chamber was obtained by weighing the fuel tank before it went in and after it came out. The actual total fuel used was 0.197 lbm. The order of magnitude difference in fuel can only be explained by a leak.

CONCLUSIONS

1. The impulse and thrust derived from the solid sublimating propulsion device did not deteriorate in any way due to the extended storage period of 8 months. The thrust data indicated that the system met the original design specifications very well.

2. There is a corrosion problem when high concentrations of ammonium hydrogen sulfide fuel are allowed to remain in contact with certain materials for extended periods. This led to the failure of the valve. Materials incompatible with this particular fuel, such as brass and copper, could not be used with this propulsion system where they may come into contact with the fuel vapors. There is some evidence to the effect that the corrosion may be predicated upon the existence of moisture or air in which case the problem may be alleviated in outer space.

3. The concept of spacecraft control devices utilizing the solid sublimating fuel as a means for propulsion is very feasible and attractive. Assuming installation of a proper valve, the attitude control system utilizing the solid sublimating fuel as the propulsion means is ready for the transition to flight hardware.

ACKNOWLEDGMENTS

The author is indebted to Mr. Michael E. Maes of Rocket Research Corporation and Dr. J. V. Fedor of GSFC for their advice and consultation concerning the rocket operation and analysis of the test data.

The author is also indebted to Messrs. James H. Kauffman and Donald J. Zbrosky for their work in setting up the instrumentation and their assistance in monitoring the actual tests.

(Manuscript received March 31, 1965)

Appendix A

The Integrating Microthrust Balance

The Integrating Microthrust Balance, IMB, is a commercially developed and produced device for accurately measuring the jet performance of very low thrust jet reaction control systems both in the steady state and pulsed operating modes. The contractor who developed the balance and calibration techniques was Rocket Research Corporation. This Appendix will describe the IMB, show its principles and procedures for use, and develop formulas for correcting the IMB data output when extended pulses are measured with damping in the system.

General Description

The IMB basically is a rectangular testing platform supported at the four corners by very weak springs such that the platform takes on the characteristics of a pendulum. Figure A1 illustrates the main components.

The microthrust balance uses a *soft* suspension to measure the momentum imparted to it by a single jet pulse. A linear displacement pendulum concept is employed, which is capable of measuring thrust impulse durations from less than 10 milliseconds up to 350 milliseconds with an overall accuracy of better than 2.0%. When the propulsion system to be tested is pulsed, the total impulse is absorbed by the balance which then deflects in proportion to this impulse and then continues to oscillate back and forth. The initial amplitude of this oscillation is directly proportional to the delivered impulse. The relative displacement is therefore measured remotely by an optical displacement detector. By calibrating the pendulum balance for relative displacement versus known values of impulse, the impulse delivered from a propulsion system may be obtained simply by recording its relative displacement and utilizing the momentum versus relative displacement calibration curve.

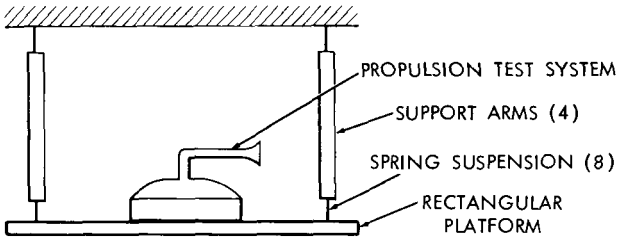

Figure A1–Side view of integrating microthrust balance.

Basic Principles

There are certain assumptions paramount for the ideal operation of this *soft* balance. They are:

1. The friction and other damping mechanisms acting on the balance are negligible with respect to the inertial forces, so that, within the desired accuracy, the balance may be treated as an undamped system.

2. The impulse is delivered to the balance rapidly enough so that negligible displacement occurs during the thrust period.

3. The supporting springs have a mass much smaller than the mass of the balance.

4. The platform and thrust mount located on it have a very high spring constant compared to the mounting springs.

5. The spring constant and mass of the system remain constant during the pulse measurement.

If the requirements above are met, the mass-spring system motion is described by the following simple equations. These are:

$$F\Delta t = mv ,$$

where

F = motor thrust,

Δt = pulse duration,

m = balance mass,

and

v = balance velocity.

After the pulse is applied the balance has a velocity and therefore a kinetic energy ($1/2\ mv^2$). This kinetic energy is ultimately all stored as potential energy of the mounting springs at maximum deflection according to the relation,

$$1/2\,mv^2 = 1/2\,kx^2 .$$

Solving for momentum,

$$mv = x(mk)^{1/2} ,$$

where

k = effective spring constant of the balance pendulum

and

x = deflection of the balance pendulum.

Since m and k remain constant for a given test set-up, it is seen that the balance deflection, x, varies directly with the balance momentum, mv.

Calibration of the Balance

For the tests described in this paper, the following calibration of the IMB was conducted. With the test system on the balance and the entire setup inside a vacuum chamber at 2×10^{-2} mm of mercury, known values of momentum were applied to the balance and the resultant relative displacements recorded. The momentum applied was accurately determined by measuring the velocity of a ball which was propelled at and captured by the balance pendulum. By

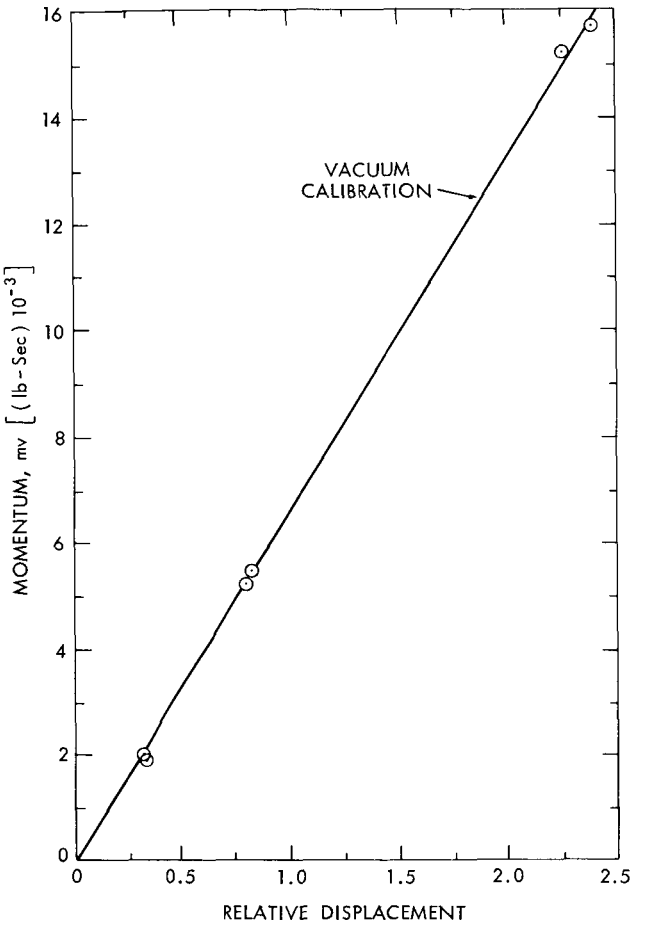

Figure A2—Calibration curve showing momentum versus displacement.

knowing the ball weight, the applied momentum, mv, was obtained. Six balls or vacuum calibration points were recorded. The calibration curve for the test is illustrated in Figure A2.

Finite Pulse Bits With a Damped System

For processes where all five assumptions previously mentioned are valid, the impulse delivered by any pulse would be that obtained from entering the calibration curve at the corresponding displacement. However, the actual conditions encountered during this test differed from the ideal case in two respects. First, the pulse duration and suspension length were such that it was impossible to impart all of the impulse to the balance before a finite displacement occurred. Second, the balance pendulum motion was damped by allowing a paddle under the pendulum to hang in a fixed pot which was filled with 20,000 centistoke silicone oil. The effect of these two conditions was to slightly reduce the balance deflection for any given impulse and thus introduce a small error. However, by manipulation of the equations of motion governing these phenomena, a correction curve may be developed by which the indicated impulse may be adjusted or corrected for any finite pulse. The following treatment is the development of the correction curve.

To develop a correction curve the approach will be to derive the two expressions describing the maximum displacement for the two processes involved; that is, first, for the ideal case balance displacement, x_{max_i}, when all of the momentum is imparted to the damped balance prior to any displacement and then, second, for the maximum balance displacement, x_{max}, when the balance pendulum is displaced and moving while the momentum is being applied. Then for any given pulse duration the ratio of x_{max}/x_{max_i} will indicate the correction necessary to the actual pendulum displacement to indicate the true total momentum applied.

The equation of motion of the spring-mass system with damping is

$$m\ddot{x} + c\dot{x} + kx = F(t) , \qquad \text{(A1)}$$

where

m = effective mass of the balance pendulum

c = damping of the balance pendulum

k = effective spring constant of pendulum

x = displacement of the balance pendulum

$\dot{x}$ = velocity of the balance pendulum

$\ddot{x}$ = acceleration of the balance pendulum

and

$F(t)$ = forcing function dependent on time.

When all of the momentum is imparted to the balance prior to any displacement, the forcing function, $F(t)$, is an impulse function at t equal zero. The solution of the linear differential equation for the complimentary function then yields the expression describing the pendulum motion:

$$x = e^{-pt} \frac{V_0}{q} \sin qt \ , \tag{A2}$$

where

t = time,

V_0 = initial pendulum velocity, $\dot{x}$, at $t = 0$,

$p = c/2m$ (a substitution made for simplicity throughout this Appendix),

$q = 1/2m \sqrt{4km - c^2}$ (a substitution made for simplicity throughout this Appendix).

By differentiating Equation A2 and setting the result equal to zero, the time, t, for the maximum displacement is obtained. Substituting this back into Equation A2, yields an expression for the ideal case maximum pendulum displacement, x_{max_i}, which is

$$x_{max_i} = \frac{V_0}{\sqrt{p^2 + q^2}} e^{-(p/q)\sin^{-1}\left(q/\sqrt{p^2+q^2}\right)} \tag{A3}$$

$$= \frac{V_0}{\omega_n} e^{-(p/q)\sin^{-1}(\omega_d/\omega_n)} \ , \tag{A4}$$

since

$\omega_n = \sqrt{p^2 + q^2}$ = undamped natural frequency of the balance pendulum,

and

$\omega_d = q$ ▫ damped natural frequency of the balance pendulum.

Now it is necessary to derive the expression for maximum displacement, x_{max}, when the thrust of the rocket, $F(t)$, is spread over a finite time period.

As the jet pulse width increases, the forcing function $F(t)$ can be approximated with good accuracy by a pulse of constant amplitude. That is, since the thrust rise and decay transients are on the order of a few milliseconds each for pulse widths in the range between 50 and 350 milliseconds, $F(t)$ can be effectively approximated by a single square-wave pulse.

For pulse widths in the range of 10 to 50 milliseconds, the pulse duration is sufficiently short with respect to the balance natural frequency that the assumption of negligible displacement during the thrust period is a good one, and the solution given by Equation A4 is valid.

For extended thrust periods, the general solution to the differential Equation A1 is found to be

$$x = \frac{F}{k}\left[1 - e^{-pt}\left(\cos qt - \frac{p}{q}\sin qt\right)\right], \tag{A5}$$

where

F = thrust of the rocket.

For an extended thrust period (i.e., F = constant) of time, t_i, followed by the thrust going to zero (i.e., $F \rightarrow 0$), the displacement expression is solved to be

$$x = e^{-pt'}\left[\frac{V_1 + py_1}{q}\sin qt' + x_1 \cos qt'\right], \tag{A6}$$

where

t_1 = thrust pulse duration

$t = t_1 + t'$ or t' = the time initiating at instant t_1 when $F \rightarrow 0$,

x_1 = balance pendulum displacement at instant, t_1,

and

V_1 = balance pendulum velocity at instant, t_1.

By maximizing Equation A6 the expression for the damped extended pulse displacement is obtained; that is,

$$x_{max} = e^{-(p/q)\sin^{-1}D}\left[\left(\frac{V_1 + px_1}{q}\right)D + x_1\left(1 - D^2\right)^{1/2}\right], \tag{A7}$$

where

$$D = \frac{1}{\sqrt{1 + \left[\frac{p}{q} + \frac{x_1 \omega_n^2}{V_1 q}\right]^2}} \tag{A8}$$

It is obvious that expressions for x_1 and V_1 must be developed to evaluate Equation A7. The expressions for x_1 and V_1 are derived by utilizing the extended thrust Equation A5 and evaluating it at $t = t_1$; i.e., at $t = t_1$, $\dot{x} = V_1$, therefore,

$$x_1 = \frac{F}{k}\left[1 - e^{-pt_1}\left(\cos qt_1 + \frac{p}{q}\sin qt_1\right)\right] \tag{A9}$$

and

$$V_1 = \frac{F}{k}\left(\frac{\omega_n^2}{q}\right)e^{-pt_1}\sin qt_1 \ . \tag{A10}$$

We have now derived the two expressions, x_{max_i} and x_{max}, which describe pendulum displacement for the two processes in question. Their ratio is

$$\frac{x_{max}}{x_{max_i}} = e^{p/q\left[\sin^{-1}(\omega_d/\omega_n) - \sin^{-1}D\right]}\left(\frac{\omega_n}{\omega_d}\right)\left[\frac{mV_1 D}{Ft_1} + \frac{mpx_1 D}{Ft_1} + \frac{x_1 \omega_d m}{Ft_1}\left(1 - D^2\right)^{1/2}\right] \tag{A11}$$

Inspection of Equations A8, A9, A10, and A11 reveals that all quantities are either easily measured parameters of the balance pendulum or are cancelled out when x_1, V_1, and D are substituted into Equation A11.

By inserting all known quantities into the four equations, a correction curve was developed which described the finite pulses on our damped system. The curve is shown in Figure A3. Inspection of the equations and the correction curve indicates that the error in displacement for finite pulse durations on any given test set-up is directly dependent upon the pulse duration only. Therefore, for a given pulse of duration, Δt_a, the correct delivered impulse was obtained by the following procedure. The relative balance displacement, S_a, was recorded. By entering Figure A2 at S_a, the uncorrected impulse, I_{unc}, on our damped balance was obtained. Then by entering Figure A3 at Δt_a, the analytical correction constant, R, for our damped finite pulse was read off. The true total impulse, I_{tot}, delivered by the finite pulse was then,

$$I_{tot} = \frac{I_{unc}}{R} \tag{A12}$$

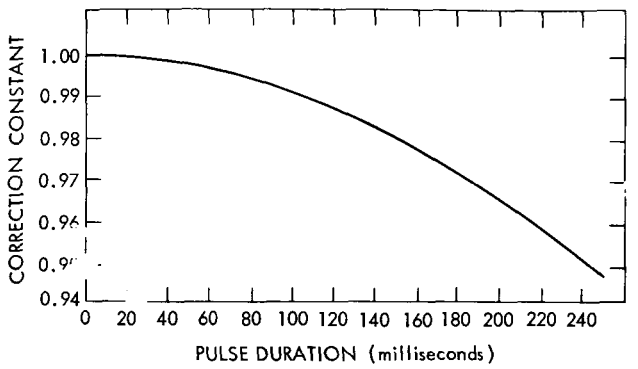

Figure A3—Finite-pulse correction curve showing correction constant versus pulse duration.

It should be noted that a much simpler correction formula may be obtained if damping is neglected in the entire analysis. For the damped system on which our tests were performed, the correction curve developed by neglecting damping would be only slightly different from Figure A3. If, however, the damping is such that there is a significant difference between the damped natural frequency, ω_d, and undamped natural frequency, ω_n, then the equations developed in this Appendix may be utilized to obtain the correct impulse delivered by the finite pulse on the damped system.

Steady State Thrusts

An equivalent system to describe steady state thrusts on the pendulum balance will now be developed. From the energy balance describing sinusoidal balance motion, that is,

$$1/2\, mv_{max}^2 = 1/2\, kx_{max}^2 ,$$

the following relationship may readily be developed which correlates the sinusoidal displacement resulting from an applied momentum to an *equivalent* displacement which would result from an *equivalent* steady state force system.

$$mv = \frac{F}{\omega_n} , \qquad \text{(A13)}$$

where

F = a steady state thrust only

and

ω_n = undamped natural frequency of the balance.

Equation A13 indicates that the resultant displacement of the balance from a steady state thrust, F, is equal to the maximum balance displacement by an ideally applied momentum (mv applied before initial displacement of balance) where the momentum is numerically equal to F/ω_n. Since the balance calibration curve is linear, it is only necessary to know the momentum applied and resultant maximum displacement at one point; from this any steady state thrust displacement may be utilized to solve for the thrust, F. Thus, the steady state thrust was obtained by the following procedure.

1. Figure A2 was entered at any displacement and the corresponding momentum read, i.e., for $S_1 = 1.5$, $mv = 0.01$ lbf-sec.

2. An equivalent steady state thrust, F_{eq}, was calculated which would result in the same displacement, $S_1 = 1.5$, i.e.,

$$F_{eq} = mv\omega_n = (0.01 \text{ lbf-sec}) \left(4.5 \frac{\text{rad}}{\text{sec}}\right)$$

$$= 0.045 \text{ lbf} .$$

3. For small displacements,

$$\frac{F}{x} = k = \text{constant} ,$$

and we have

$$k = \frac{.045}{1.5} = 0.03 .$$

4. Therefore, with our particular test set-up, for any steady state thrust, F_a, and the resultant displacement, S_a, the thrust was

$$F_a = 0.03 \left(S_a\right) .$$

As an example, if S_a equaled 1.40, then

$$F_a = 0.042 \text{ lbf} .$$

Appendix B

List of Symbols

A_t = Throat area of the test rocket

c = Damping of the balance pendulum

C_f = Thrust coefficient of the test rocket

c_f = Specific heat of the fuel

c_t = Specific heat of the fuel tank

F = Thrust from test rocket

h_{sg} = Heat of sublimation of the fuel

I_{sp} = Specific impulse of the fuel

k = Thrust coefficient of the test rocket

m = Thrust balance mass

P_c = Absolute tank chamber pressure

Q = Total heat exchanged

T = Temperature

t = Time

w_f = Weight of fuel

$\dot{w}_f$ = Weight of fuel used per unit time

w_t = Weight of the fuel tank

x = Thrust balance lateral displacement

$\dot{x}$ = Thrust balance lateral velocity

$\ddot{x}$ = Thrust balance lateral acceleration